An Image Segmentation Assessment Tool ISAT 1.0

Anton Mazhurin[1] and Nawwaf Kharma[2]

[1]*ALMAZ Technology, 1790 du Canal, 302, Montreal (QC), H3K 3E6, Canada*

[2]*Department of Electrical & Computer Engineering, Concordia University, Montreal (QC), H3G 1M8, Canada*

Keywords: Image Segmentation, Quality Assessment, Software Tool, Pixel-based Measures, Region-based Measures.

Abstract: This paper presents algorithms and their software implementation, which assess the quality of segmentation of any image, given an ideal segmentation (or ground truth image) and a usually less-than-ideal segmentation result (or machine segmented image). The software first identifies every region in both the ground truth and machine segmented images, establishes as much correspondence as possible between the images, then computes two sets of measures of quality: one, region-based and the other, pixel-based. The paper describes the algorithms used to assess quality of segmentation and presents results of the application of the software to images from the Berkeley Segmentation Dataset. The software, which is freely available for download, facilitates R&D work in image segmentation, as it provides a tool for assessing the results of any image segmentation algorithm, allowing developers of such algorithms to focus their energies on solving the segmentation problem, and enabling them to tests large sets of images, swiftly and reliably.

1 MOTIVATION & REVIEW

Many researchers develop, extend and apply algorithms for image segmentation. A natural part of their work is the assessment of the quality of the results achieved by the segmentation algorithm. Most day-to-day assessment work, during the development stage is done by eye, with more rigorous computerized evaluations carried out towards the end of the development cycle, using in-house scripts or programs that are almost always pixel-based, and still require a fair amount of manual labelling. Now, this may be acceptable if the entity doing the development is human, but is impossible if one intends to utilize an automated method for image segmentation program development, such as genetic programming (Singh, 2009).

Hence, for reasons of (a) freeing researchers and developers from the task of building their own image segmentation quality assessment tool; (b) providing the community with not just pixel-based but also region-based measures that (c) do not require manual labelling of the various regions of the image, and in a package that (d) can provide an objective function for automated development applications, for all the above reasons, we have specified and developed ISAT 1.0.

In the literature, there is hardly any immediately usable software tools dedicated to the automated assessment of mage segmentation results, from both pixel- and region-based perspectives, a tool that only requires edge-images of the machine segmented result and the human generated ground truth, and without any need for region marking.

There are, however, a large number of related publications worthy of note. They include the work by (Francisco, 2009), (Jiang, 2006), (Cardoso, 2005) and most recently, (McGuiness, 2011). These and others use approaches that all come under two mutually exclusive categories: *objective* evaluation methods that do not involve a human operator and *subjective* assessment methods that do (Zhang, 2008). Of the objective evaluation methods, only empirical methods assess the quality of segmentation by *direct* evaluation of the resulting segmented images, and they do so in either *supervised* or *unsupervised* ways. Unsupervised means of segmentation quality evaluation do not require a ground truth image, but decide the quality of segmentation based on the presence of certain characteristics normally associated with properly segmented images (Unnikrishnan, 2007). These methods have their advantages, as they allow automated evaluation of a large number of segmented images without the laborious effort needed for manual production of a large number of

Mazhurin A. and Kharma N..
An Image Segmentation Assessment Tool ISAT 1.0.
DOI: 10.5220/0004216404360443
In *Proceedings of the International Conference on Computer Vision Theory and Applications* (VISAPP-2013), pages 436-443
ISBN: 978-989-8565-47-1

matching ground truth images. However, it is well-known that that such an approach will often fail under conditions where the required segmentation is related to the meaning of the segmented image. Indeed, if a reliable unsupervised objective method had existed then it would have formed the basis of one of the best (if not the best) image segmentation algorithms to date. That is not the case. Hence, researchers still utilize either subjective evaluation, which requires ground truth or supervised objective evaluation, which also requires ground truth. Our method comes under supervised means of objective evaluation, and it is assessed – as it ought to be – by subjective visual inspection.

2 METHODOLOGY

ISAT assesses the quality of segmentation of any image. To do so, ISAT does not require the original image, but two other images representing the ideal and actual segmentation of the original image. As a matter of terminology, the ideally segmented image, which is usually drawn by hand, is called the *ground truth* image (or GT). The other image represents the result of a segmentation procedure, which is usually executed by machine, and is called the Machine Segmented image (or MS). Both of these images are binary images, in that they exhibit the boundaries of the segmented regions as black curves on a white background. In all following calculations, it is the GT that functions as a reference of presumed truth against which a MS image is judged.

To carry out any kind of segmentation quality assessment, connected regions in both GT and MS images must be established then, crucially, every region in GT must – if possible – be matched with one or more regions in MS. Note that one region in GT may match one region in MS; that region in GT would then be *correctly* segmented if the overlap between the two regions is great enough or *missed* if the overlap is insufficient. Also, more than one region in GT may be matched with one region in MS; that region in GT would be *under-segmented*. On the other hand, multiple regions in MS may correspond to one region in GT; that region in GT would then be *over-segmented*. Finally, every region that exists in MS but does not correspond to any region(s) in GT is considered *noise*. Region-based accuracy is calculated as a ratio of the number of correctly matched regions in MS to the sum of all the regions in GT, plus the number of noise regions (which come from MS). All of the above measures were based on equivalent measures proposed by Hoover *et al.* (Hoover, 1996).

As such, an ideally segmented image, from a region-based perspective, entails that every region in GT is exclusively matched with exactly one region in MS, with zero noise (i.e., unmatched regions in MS). And in fact, ISAT will return a region-based accuracy of 100%, for this case. Note that matching requires an overlap between the two matched regions exceeding a pre-set threshold, which we currently set to 66% and should not be set to 100%. This ensures that the number of correctly segmented regions reflects human conceptions of region-based segmentation, where the *number* of approximately matched regions (e.g., red blood cells) matter more than the precise *fit* of every matched region (e.g., one blood cell).

Once region identification in both GT and MS is completed, and matching of regions between GT and MS is done, it is possible to compute all region-based segmentation quality measures. But also, this makes it possible to compute the other set of pixel-based segmentation quality measures. These measures sound familiar, but they are applied differently than the well-known *True Positive*, *False Negative*, *True Negative* and *False Positive* measures used in innumerable studies in image processing (Bushberg, 2002). We will describe the final pixel-based measures here intuitively, as the following sub-sections describe all the measures, in full detail. In brief, the final pixel-based measures provide a normalized image-wide quantitative assessment of the quality of the fit between the regions of GT and those they were matched with in MS. As such, our *sensitivity* is the percentage of pixels of regions of GT that were matched with regions in MS. *Specificity* is the percentage of pixels of the backgrounds of the various regions in GT that were in fact assigned to backgrounds of the matching regions in MS. We define the background of a region as those pixels that belong to the image but not to that region, and we exclude the pixels of the edges between regions from all calculations.

An ideally segmented image, from a pixel-based perspective is similar to an ideally segmented image, from a region-based point of view, but for one exception. Using the red blood cells example, every blood cell boundary in the MS image must fit perfectly the boundary of every corresponding blood cell in the GT image; any deviation no matter how small will reduce either sensitivity or specificity and hence the overall pixel-based measure of accuracy, which is a weighted average of the two.

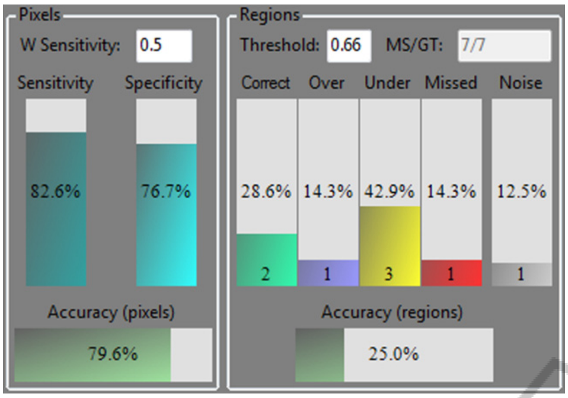

Pixels

W Sensitivity: 0.5

Sensitivity 82.6%

Specificity 76.7%

Accuracy (pixels) 79.6%

Regions

Threshold: 0.66

MS/GT: 7/7

Correct	Over	Under	Missed	Noise
28.6%	14.3%	42.9%	14.3%	12.5%
2	1	3	1	1

Accuracy (regions) 25.0%

Figure 1: The results window in ISAT 1.0.

2.1 Region-based Measures

First, ISAT enumerates and marks all connected regions in both GT and MS images. The number of pixels in every region is also computed and stored. The pixels that make-up the boundaries of the regions are eliminated from the calculations, as they do not belong to any region. Let *N* be the number of regions in the GT image and *M* be the number of regions in the MS image. Let the number of pixels in each GT region R_n be called P_n (where $n = 1... N$). Similarly, let the number of pixels in MS region R_m be called P_m (were $m = 1… M$). An *overlap table* with size $N\times M$ is calculated. Every cell $O_{n,m}$ in the overlap table contains the number of pixels in the overlapping area of the two corresponding regions R_n and R_m. If the two regions do not overlap then the value $O_{n,m}$ will be zero. If there is a perfect match between the two regions then $O_{n,m} = P_n = P_m$.

Second, a classification procedure marks every region as a member of one of the five exclusive groups: *correct*, *over-segmented*, *under-segmented*, *missed* and *noise*. The classification procedure uses a single input parameter threshold *T*. This parameter defines the strictness of all group classifications; the default value is 0.66 (~2/3). Classification rules for every group follow (consult Figure 2).

- *Correct*: GT region R_n and MS region R_m are marked as *correct* IFF
  (a) at least *T* percent of GT region R_n overlaps with region R_m. This can be expressed as:

  $$O_{n,m} >= T \,.\, P_n \qquad (1)$$

  AND
  (b) at least *T* percent of MS region R_m overlaps with region R_n, formulaically expressed as:

  $$O_{n,m} >= T \,.\, P_m \qquad (2)$$

- *Over-segmented*: GT region R_n and a set of MS regions R_{m1}... R_{mx} (were $2 <= x <= M$) are marked *over-segmented* IFF
  (a) for every MS region R_{mi} in the set (where $i = 1... x$), at least *T* percent of that region overlaps with GT region R_n. Also, expressed as:

  $$O_{n,mi} >= T \,.\, P_{mi} \qquad (3)$$

  AND
  (b) at least *T* percent of GT region R_n overlaps with the union of the set of MS regions. This is expressed as:

  $$\sum_{i=1}^{x} O_{n,mi} >= T \,.\, P_n \qquad (4)$$

- *Under-segmented*: MS region R_m and a set of GT regions R_{n1}... R_{nx} (were $2 <= x <= N$) are marked as *under-segmented* IFF
  (a) for each GT region R_{ni} in the set (where $i = 1... x$), at least *T* percent of that region overlaps with MS region R_m. This can be expressed as:

  $$O_{ni,m} >= T \,.\, P_{ni} \qquad (5)$$

  AND
  (b) at least *T* percent of MS region R_m overlaps with the union of the set of GT regions, also expressed as:

  $$\sum_{i=1}^{x} O_{ni,m} >= T \,.\, P_m \qquad (6)$$

- *Missed*: a GT region R_n is marked as *missed* if it has not been marked as *correct*, *over-segmented* or *under-segmented*.

- *Noise*: a MS region R_m is marked as *noise* if it has not been marked as *correct*, *over-segmented* or *under-segmented*.

After the regions are classified, we normalize the numbers of regions in every group using the following rules; this results in percentages.

- for *correct* regions: the number of GT regions marked as *correct* is divided by the total number of GT regions.

- for *over-segmented* regions: the number of GT regions marked as *over-segmented* is divided by the total number of GT regions.

- for *under-segmented*: the number of GT regions marked as *under-segmented* is divided by the total number of GT regions.

- for *missed* regions: the number of GT regions marked as *missed* is divided by the total number of GT regions.
- However, for *noise* regions: the number of MS regions marked as *noise* is divided by the sum of (a) the number of MS regions marked as *noise* plus (b) the total number of GT regions.

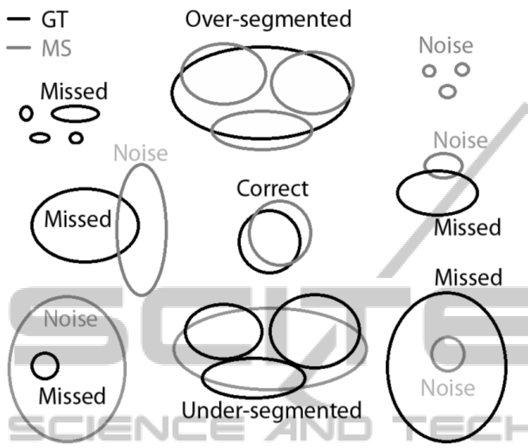

Figure 2: All possible classifications of regions in a GT and corresponding MS image (if any).

The accuracy value of the region-based measures (*AccuracyR*) is calculated as the ratio of number of *correct* regions to the sum of (a) the total number of GT regions and (b) the number of noise regions.

$$AccuracyR = NumCorrect / (N + NumNoise) \quad (7)$$

N is the total number of GT regions;*NumCorrect* is number of correct regions; *NumNoise* is the number of noise regions.

2.2 Pixel-based Measures

For every *match* between one or more GT regions with one or more MS regions, and for every GT and MS region that is *un-matched*, four basic values are computed (some returning zero values): *True Positive* (TP), *False Negative* (FN), *True Negative* (TN) and *False Positive* (FP). This results in individual results that must be summed up, before image-wide *overall* TP, FN, TN and FP can be calculated.

In more detail (see Figure 3), one GT region could match exactly one MS region (giving us a 'correct' group); one GT region could match more than one MS region (giving us an 'over-segmented' group of pixels) and conversely one MS region could match more than one GT region (giving us an 'under-segmented' group of pixels). Finally, there are regions in GT that are not matched with any MS region (the 'missed' group) and MS regions that are not matched with any GT regions (the 'noise' group). It is important to underline the fact that the following calculations provide us with a whole set of TP, FN, TN and FP numbers that must be summed up, before *overall* image-wide figures for TP, FN, TN and FP can be secured. It is those overall values that are used to compute *specificity* and *sensitivity*, then *pixel-based accuracy.*

So, to begin with, for every matched and un-matched region in GT and MS, the following individual TP, FN, TN and FP values are computed, according to the following rules.

- *True Positive.* TP relies on one source:
  (a) *Correct* group: the number of pixels in the overlap area of GT region R_n and MS region R_m.

$$TP = O_{n,m} \quad (8)$$

- *False Negative*. FN comprises the number of pixels from four different groups:
  (a) *Correct* group: the number of pixels in GT region R_n which are not in an overlap area with MS region R_m.

$$FN_{correct} = P_n - O_{n,m} \quad (9)$$

  (b) *Other* groups, comprising of *over-segmented*, *under-segmented* and *missed* groups. This is the number of pixels in GT regions.

$$FN_{other} = P_n \quad (10)$$

  FN is the sum of $FN_{correct}$ and FN_{other}.

- *True Negative*. TN relies on one source, but involves a necessary normalization.
  (a) *Correct* group: the calculation is performed in two steps in order to avoid dependence on image dimensions. First, the normalized value TN_{norm} is calculated as a ratio of (a) the number of actual TN pixels (the number of pixels in the image which are not in GT region R_n AND not in MS region R_m) to (b) the maximum possible number of TN pixels for this region (equals the number of pixels in the image which are not in GT region R_n). This is expressed as:

$$TN_{norm}= (N_{total} – (P_n + P_m – O_{n,m})) / (N_{total} - P_n) \quad (11)$$

  Note that N_{total} is the number of pixels in the image. Second, the value of TN_{norm} is weighted by the number of pixels in GT region R_n:

$$TN = TN_{norm} . P_n \quad (12)$$

- *False Positive*. FP comprises the total number of pixels belonging to four groups:

  (a) *Correct* group: the calculation is performed in two steps in order to reflect the normalization of the complimentary value of TN (see (11) and (12)). First, the normalized value FP_{norm} is calculated as a ratio of (a) the number of actual *FP* pixels (the number of pixels in MS region R_m which are not in the overlap area with GT region R_n) to (b) the maximum possible number of *FP* pixels for this region (the number of pixels in MS region R_m).

  $$FP_{norm} = (P_m - O_{n,m}) / P_m \quad (13)$$

  Second, the value of FP_{norm} is weighted by the number of pixels in GT region R_n:

  $$FP_{correct} = FP_{norm} \cdot P_n \quad (14)$$

  (b) *Other* groups, comprising of *over-segmented*, *under-segmented* and *noise* groups. This is the number of pixels in MS regions.

  $$FP_{other} = P_m \quad (15)$$

  FP is the sum of $FP_{correct}$ and FP_{other}.

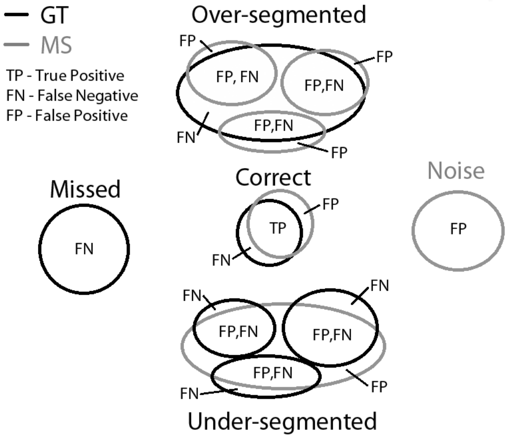

Figure 3: All possible classifications (except TrueNegative) of pixels in an MS region, relative to its corresponding GT regions.

As stated above, once all four values are calculated for the various matched and unmatched regions in GT and MS, the individual TP, FP, TN and FP figures are summed up, and the resulting *Overall TP*, *Overall FP*, *Overall TN* and *Overall FP* values are used in the formulas to calculate sensitivity, specificity and accuracy. Note that W_{sens} is the weight assigned to sensitivity, which takes a value in the range of [0,1] with its default set to 0.5.

$$\textit{Sensitivity} = (\textit{Overall TP}) / (\textit{Overall TP} + \textit{Overall FN}) \quad (16)$$

$$\textit{Specificity} = (\textit{Overall TN}) / (\textit{Overall TN} + \textit{Overall FP}) \quad (17)$$

$$\textit{AccuracyP} = W_{sens} \,.\, \textit{Sensitivity} + (1 - W_{sens}) \,.\, \textit{Specificity} \quad (18)$$

3 APPLICATION NOTE

ISAT 1.0 installation package for Win32 platform is currently available for free download at www.ece.concordia.ca/~kharma/ExchangeWeb/ISA.

The package is a fully functional application with a GUI. It can be used in various image segmentation tasks as is. Additionally, it has C++ and C# APIs that allow for its use as a library, by other programs.

The user has to specify three folders for Original images, GT images and MS images. ISAT enumerates all the images in the folder, and it automatically matches Original, GT and MS images using a simple rule: the names of both GT and MS image files have as prefix the name of the corresponding original image file. The installation package contains a set of sample images.

ISAT displays all three images (original, GT and MS) in a single window on top of each other, and enables control of the opacity of every image for visual evaluation of segmentation quality.

ISAT supports all major image formats and is also able to read the special '.seg' file format used by the Berkeley Segmentation Dataset and Benchmark or BSDB (Berkeley, 2012).

4 RESULTS

To evaluate our methodology through the application of ISAT 1.0, we make use of the well-known Berkley Segmentation Dataset and Benchmark picked a few examples to exhibit how well the results reflect human conceptions of segmentation quality, within bounds of theoretical correctness. By that, we mean (a) MS images that generate ideal or near-ideal segmentation results should give perfect or near-perfect accuracy results, respectively; (b) MS images that exhibit over-segmented or under-segmented regions should respectively have over- and under-segmentation results that reflect that fact; (c) MS images that identify non-existing regions or miss some regions in GT altogether, should have that noted in elevated missed and noise values. In addition, (d) images with identical region-based measures that differ – even a little – in precision of fit, between MS and corresponding GT regions, should have different pixel-based measurement values.

The first example is shown in Figure 4. The first row has the original image on the left and the GT image on the right. The first MS image is the second one from the top. It obviously is greatly under-segmented and is missing a large number of GT regions, but suffering little noise. This is reflected in the measures on the left-hand side, as under-segmentation is at 65.2% while over-segmentation is zero, correctly identified regions is low at 6.1% while 28.8% of GT regions were completely missed. This MS image gives an overall region-based accuracy of 5.8% and a larger pixel-based accuracy of 41.4% (due to the large size of the four regions that were correctly segmented). Going down the right column, we see another MS image with well-identified petals and nothing else, taking down region-based accuracy to 2 regions (or 3%) and reducing pixel-based accuracy to 38%. This is followed by the last MS image with a deservedly low pixel-based accuracy of just 17.6%.

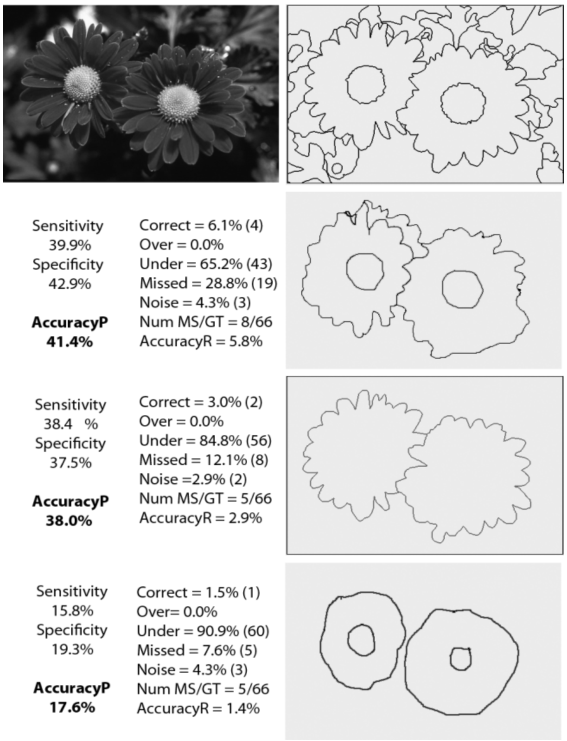

Figure 4: The original image of two flowers (BSDB training image #124084) and the ground truth image, followed by three segmentation results with decreasing levels of quality.

The second example shows the face of a woman. Again, the first row has on the left the original image, which does not enter into processing, and on the right the ideal or GT image. Each of the second, third and fourth rows have on the right an MS image and on the left the results of comparing that image to the GT using ISAT. It is clear to the naked eye that the quality of segmentation decreases from top to bottom. The first segmentation result (second row) is almost as good as the GT, except that it under-segments and misses altogether a few regions that appear in GT; it also introduces regions that have no equivalent in GT. This reflects itself in a significant under-segmentation score of 14.5% and high values for both missed (48.4%) and noise (27.1%) measures of region-based segmentation quality. All in all, region-based accuracy is 27.1%, as only 23 of the GT's 62 regions were correctly matched. On the pixel-based front, sensitivity and specificity for the higher figures are higher (at 86.3% and 63% vs. 12% for the lowest MS).

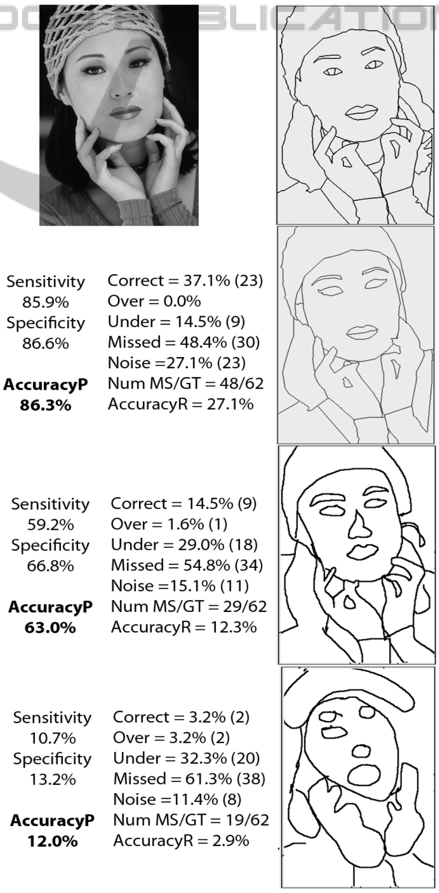

Figure 5: The original image of a woman (BSDB training image# 302003) and the ground truth image, followed by three segmentation results with decreasing levels of quality.

Figure 6 presents a structure, with a rather simplified ideal or GT image. As with the preceding examples, the first row contains the original image (left) and the ideal segmentation (right). The other rows have an MS image (right) next to the segmentation quality data (left) coming from ISAT's comparison of the MS image to the GT image. The first result in the second row shows what appears to be near-perfect segmentation, yielding a pixel-based accuracy of 97.6%. Closer inspection, however, reveals a number (5) of tiny regions in the MS image that do not correspond to any regions in GT. This is the reason for the elevated noise value of 55.6% and hence low region-based accuracy of 44.4%. Skirting that anomaly, correctness returns a value of 100%, as all regions in GT have matching regions in the MS image.

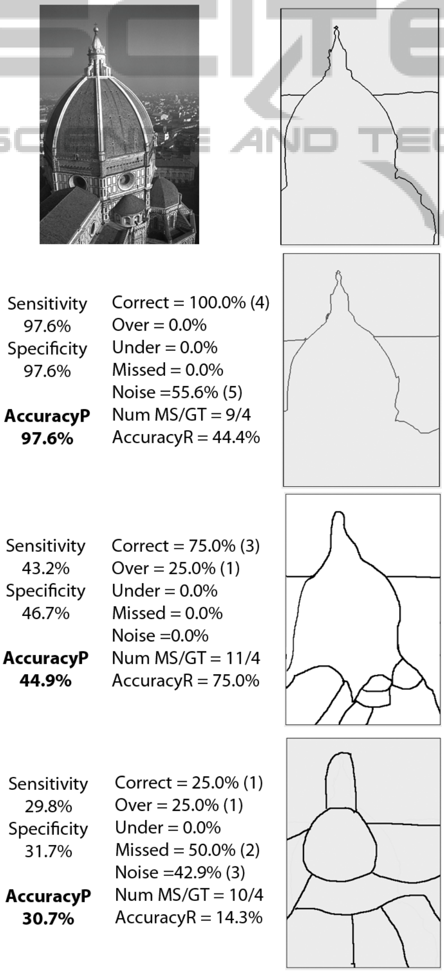

Figure 6: The original image of a structure (BSDB training image #24004) and the ground truth image, followed by three segmentation results with decreasing levels of quality.

Going down to the third row in Figure 6, one can identify a few regions in the MS image, which do not have equivalents in GT. This reflects a significant degree of over-segmentation, which is at 25%. As a result of this over-segmentation, region-based accuracy is diminished by the same amount, down to 75%. Finally, noise appears to have gone down to zero, but that is only because this MS image (which is hand-drawn by the first author) does not have the minute pockets of ghost regions that were part of the automatically segmented MS in the second row. Finally, the last row in Figure 6 exhibits the worst segmentation results reflected in the worst region- and pixel-based accuracy results of 14.3% and 30.7%, respectively.

It is worth noting that we actually were able to run all the images in the Berkeley Dataset, and that we did not notice any particular problems in either the operation of the program or the nature of the numerical results. In any case, ISAT 1.0 could not fail to count regions or pixels in line with the authors' specifications. It is, in the final analysis, the subjective evaluation of our readers – within theoretical limits – that decides the affinity of our segmentation measures to human conceptions of segmentation quality. Hence, we invite them to do that and provide us with feedback on ISAT's practical efficacy by downloading and testing the tool from the web-site listed in section 3.

5 CONCLUSIONS

This paper reports on a method that automatically matches regions in *ground truth* edge-images with their most-likely counterparts in corresponding *machine segmented* edge-images, as a prelude to the computation of theoretically founded *region-based* and *pixel-based* measures of segmentation quality. We are not aware of a software tool dedicated to the provision of this service; a service that almost every researcher in image segmentation needs for efficient direct quantification of the performance of his/her segmentation method *vis-a-vis* a human-generated ground truth. The region- and pixel-based results used here are theoretically founded and particularly adapted to our region-matching needs. The application of those measures (*via* ISAT 1.0) to the Berkeley Segmentation Dataset shows that the measures return values that are in tune with human conceptions of segmentation accuracy, with its various components (e.g., under- and over-segmentation). Sample results of our application are shown in section 4. We invite everyone involved in image segmentation to download and test the tool, from the web-site listed in section 3. We would be glad to respond to any reasonable suggestion for improvement.

REFERENCES

Berkley Segmentation Dataset and Benchmark, http://www.eecs.berkeley.edu/Research/Projects/CS/vision/bsds/ (last accessed: July 30, 2012).

Bushberg, J. T., Seibert, J. A., Leidholdt, E. M., Boone, J.M., 2002. The essential Physics of Medical Imaging, published by *Lippincott Williams & Wilkins, Philadelphia*, pp. 288-290.

Cardoso, J. S.; Corte-Real, L., 2005. Toward a generic evaluation of image segmentation. *IEEE Transactions on Image Processing*, vol.14, no.11, pp.1773-1782.

Francisco, E. and Jepson, A., 2009. Benchmarking Image Segmentation Algorithms. *International Journal of Computer Vision*, vol. 85, issue 2, pp. 167-181.

Hoover, A., Gillian, J.-B., Jiang, X., Flynn, P.J., Bunke, H., Goldgof, D., Bowyer, K., Eggert, D.W., Fitzgibbon, A., Fisher, R.B. 1996. An experimental comparison of range image segmentation. *IEEE Transactions on Pattern Analysis and Machine Intelligence*, vol.18, no.7, pp.673-689.

Hui Zhang, H., Fritts, J. E., Goldman, S.A., 2008. Image Segmentation Evaluation: A Survey of Unsupervised Methods. *Computer Vision and Image Understanding*, vol.110, no.2, pp. 260-280.

Jiang, X., Marti, C., Irniger, C. and Bunke, H., 2006. Distance measures for image segmentation evaluation. *EURASIP Journal on Applied Signal Processing*, vol. 2006, pp. 1-10.

McGuiness, K. and O'Connor, N. E., 2011. Toward Automated Evaluation of Interactive Segmentation. *Computer Vision and Image Understanding*, vol. 115 no. 6, pp. 868-884.

Singh, T., Kharma, N., Daoud, M. and Ward, R., 2009. Genetic programming based image segmentation with applications to biomedical object detection. *Proceedings of the 11th Annual conference on Genetic and evolutionary computation* (GECCO '09). ACM, New York, NY, USA, 1123-1130.

Unnikrishnan, R., Pantofaru, C., Hebert, M., 2007. Toward Objective Evaluation of Image Segmentation Algorithms, *IEEE Transactions on Pattern Analysis and Machine Intelligence*, vol.29, no.6, pp.929-944.